



INSTITUT DE FRANCE
Académie des sciences

Comptes Rendus

Physique

Yoshitaka Kuno and Guillaume Pignol

Precision experiments with muons and neutrons


Volume 21, issue 1 (2020), p. 121-134.

<<https://doi.org/10.5802/crphys.13>>

Part of the Thematic Issue: A perspective of High Energy Physics from precision measurements

Guest editors: Stéphane Monteil (Clermont Université, CNRS/IN2P3, Clermont-Ferrand) and Marie-Hélène Schune (Université Paris-Saclay, CNRS/IN2P3, Orsay)

© Académie des sciences, Paris and the authors, 2020.
Some rights reserved.

 This article is licensed under the
CREATIVE COMMONS ATTRIBUTION 4.0 INTERNATIONAL LICENSE.
<http://creativecommons.org/licenses/by/4.0/>



Les Comptes Rendus. Physique sont membres du
Centre Mersenne pour l'édition scientifique ouverte
www.centre-mersenne.org



A perspective of High Energy Physics from precision measurements
La physique des Hautes Energies du point de vue des mesures de précision

Precision experiments with muons and neutrons

Expériences de précision avec les muons et les neutrons

Yoshitaka Kuno^a and Guillaume Pignol^{*, b}

^a Osaka University, Machikaneyama, Toyonaka, Osaka, 560-0043, Japan

^b Univ. Grenoble Alpes, CNRS, Grenoble INP, LPSC-IN2P3, 38000 Grenoble, France.

E-mails: kuno@phys.sci.osaka-u.ac.jp (Y. Kuno), guillaume.pignol@lpsc.in2p3.fr (G. Pignol).

Abstract. The precision experiments with muons and neutrons are described. The topics selected cover the anomalies of the muon $g_\mu - 2$ and the neutron lifetime, and searches for charged lepton flavour violation CLFV of $\mu^- \rightarrow e^-$ transition and the neutron electric dipole moment (EDM). These physics programs are anticipating significant improvements of experimental sensitivities, by a factor of ten to more than 10,000 with novel ideas and methods. They would provide a unique discovery potential to new physics beyond the Standard Model of particle physics, and is complementary to the collider and neutrino physics programs.

Résumé. Une sélection d'expériences de précision employant des muons ou des neutrons sont décrites. Cette sélection couvre les anomalies dans les mesures du facteur $g_\mu - 2$ du muon et de la durée de vie du neutron, ainsi que les recherches de violation de saveur pour les leptons chargés (CLFV) des transitions $\mu^- \rightarrow e^-$ et du moment dipolaire électrique (EDM) du neutron. Ces programmes promettent des améliorations significatives de la sensibilité expérimentale, les facteurs d'améliorations sont compris entre 10 et 10,000, avec des nouvelles idées et méthodes. Le potentiel de découverte de nouvelle physique au-delà du Modèle Standard de la physique des particules est complémentaire aux recherches sur collisionneurs et aux programmes avec les neutrinos.

Keywords. Neutron, Muon, Neutron lifetime, Muon magnetic moment, Muon anomaly, Lepton flavor violation, Electric dipole moment.

Mots-clés. Neutron, Muon, Temps de vie du neutron, Moment magnétique du muon, Anomalie du muon, Violation de la saveur leptonique, Moment dipolaire électrique.

* Corresponding author.

1. Muons and neutrons at the intensity frontier

About twenty large nuclear facilities dedicated to neutron and/or muon production are presently being operated in the world. These are fission nuclear reactors producing neutrons (and neutrinos), and accelerators to make spallation sources producing neutrons, pions and muons. Concerning nuclear reactors, there are about 15 research reactors accessible to scientific users in operation. One of the world center for neutron science is the high flux 48 MW reactor at the Institut Laue Langevin in France, with a thermal flux of $10^{15} \text{ n cm}^{-2}\cdot\text{s}^{-1}$ delivering neutrons to 45 instruments in parallel. In a spallation source, a high intensity ($\sim\text{mA}$) proton beam ($\sim\text{GeV}$) is shot at a target made with heavy elements such as lead, tungsten or mercury. By destroying nuclei, spallation reactions liberate typically 20 neutrons and several pions per incoming proton. The muons are indirectly produced by the decays of pions. Large spallation sources are currently operated at Paul Scherrer Institute (PSI) in Switzerland, SNS in the US and the Japan Proton Accelerator Research Complex (J-PARC) in Japan. The European Spallation Source (ESS) is currently under construction in Sweden. Concerning muon beam facilities, there are proton cyclotrons which produce a continuous muon beam such as PSI and TRIUMF, and proton synchrotrons which provide a pulsed muon beam such as ISIS/RAL and J-PARC. The time structure of a muon beam is important and should be chosen appropriately for an experiment. Among the facilities, PSI and J-PARC can deliver a proton beam of about 1 MW power, providing good opportunities for muon particle physics.

These installations are multidisciplinary facilities. Chemists and solids state physicists make good use of the neutron or muon beams as a probe of a sample of condensed or soft matter they wish to characterize. By contrast, particle physicists study the neutron and muon themselves to do precision experiments at the intensity frontier which are of two types: metrology measurements and quasi-null tests.

- *Metrology measurements.* This class of experiments aim at an accurate measurement of a non-zero quantity. Experiments with muons in this category include the measurement of the muon lifetime τ_μ used to extract the Fermi constant, and the muon magnetic moment anomaly $(g_\mu - 2)/2$. Neutrons are obviously used to measure the neutron lifetime τ_n and the various correlation coefficients in the three-body decay of the neutron.
- *Quasi-null tests.* These aim at testing symmetries – exact or approximate – of the Standard Model. Current or planned experiments are sensitive probes of new physics, because in general the new physics could violate these approximate symmetries. With muons, one can probe charged lepton flavour violation (CLFV) processes such as the $\mu^+ \rightarrow e^+ \gamma$ decay. It is not strictly speaking a null test because neutrino oscillations violate the conservation of lepton flavor, but in the charged lepton sector the effect of the PMNS matrix is much too small to be measured, it is a quasi-null test. With neutrons, one can test baryon number conservation by measuring the neutron-antineutron oscillation. If $n - \bar{n}$ oscillation is observed, it would violate not only B conservation but also $B - L$. It is therefore a strict null test because $B - L$ is strictly conserved in the SM. Finally, the measurement of the Electric Dipole Moment (EDM) of the neutron is a test of time reversal symmetry, and therefore of CP symmetry according to the CPT theorem. Although CP violation is allowed in the SM, flavor-diagonal CP violation (the case of the EDM) is largely suppressed. The search for the neutron EDM is in fact a quasi-null test.

It is impossible to cover all aspects of precision experiments with neutrons and muons in this short review. Not only because of space limitations, but also because of the incompetence of the authors. Instead we choose to develop topics which, in our biased opinion, are the most interesting. In the second section we will report on the current status of the two persisting discrepancies (4σ), namely the disagreement between the experimental and theoretical values

for the $(g_\mu - 2)/2$, and the neutron lifetime puzzle. Sadly, we will not cover the more recent “proton radius puzzle”, in which a muon experiment play a key role. Next we will cover the CLFV processes with muons in Section 3 and the search for the neutron EDM in Section 4. To cover the gaps in this review we refer to the following review on particle physics with neutrons [1] and reviews on muon particle physics [2, 3].

2. Two persisting discrepancies

2.1. Status of the muon $(g_\mu - 2)$ anomaly

Since the muon is a Dirac particle, the g factor of its magnetic moment is two (2), when quantum corrections are not included. Here, the g factor is defined as

$$\vec{\mu} = g \frac{e}{2m} \vec{s}, \quad (1)$$

where $\vec{\mu}$ is the magnetic moment vector, \vec{s} is the spin vector, e and m are the electric charge and the mass respectively. A deviation from two, namely $(g - 2)$, arises by quantum corrections, which can be calculated precisely in the SM. They are divided into higher-order QED corrections, hadronic vacuum polarization (HVP), hadronic light-by-light (HLbL) and electroweak (EW) contributions. For instance, one of the recent updates of theoretical calculations on $a_\mu = (g_\mu - 2)/2$ for the muon [4] gives

$$a_\mu^{\text{QED}} = 11658471.90(0.01) \times 10^{-10}, \quad (2)$$

$$a_\mu^{\text{HVP}} = 684.69(2.4) \times 10^{-10}, \quad (3)$$

$$a_\mu^{\text{HLbL}} = 9.80(2.60) \times 10^{-10} \quad \text{and} \quad (4)$$

$$a_\mu^{\text{EW}} = 15.36(0.10) \times 10^{-10}. \quad (5)$$

By adding the above contributions, the SM prediction is

$$\begin{aligned} a_\mu^{\text{SM}} &= a_\mu^{\text{QED}} + a_\mu^{\text{HVP}} + a_\mu^{\text{HLbL}} + a_\mu^{\text{EW}} \\ &= 11659182.05(3.56) \times 10^{-10}. \end{aligned} \quad (6)$$

On the other hand, the present experimental value of a_μ is given by BNL E821 [5],

$$a_\mu^{\text{exp}} = 11659208.9(6.3) \times 10^{-10} \quad (\pm 540 \text{ ppb}). \quad (7)$$

The experimental value has about $+3.7\sigma$ deviation from the SM prediction. It is not known yet whether this deviation is due to new physics beyond the SM or not.

Experimentally the $(g_\mu - 2)$ is measured by the frequency (ω_a) of muon spin precession with respect to the muon momentum vector in a muon storage ring. The Larmor frequency of the muon spin precession (ω_s) and the cyclotron frequency of the muon motion (ω_c) are given respectively as follows,

$$\omega_s = \frac{eB}{m_\mu \gamma} \left[1 + \frac{g_\mu - 2}{2} \gamma \right] \quad \text{and} \quad \omega_c = \frac{eB}{m_\mu \gamma}, \quad (8)$$

$$\omega_a \equiv \omega_s - \omega_c = \frac{a_\mu eB}{m_\mu}. \quad (9)$$

A new experiment E989 at Fermilab [6] is now running to improve an accuracy by a factor of four, reaching 140 ppb. The E989 experiment utilizes the same muon $(g_\mu - 2)$ storage ring used in BNL E821 with several significant improvements on a muon beam and detectors. Another experimental program at J-PARC is under preparation (J-PARC E34) [7]. It uses a low-emittance slow μ^+ beam produced from laser ionization of a muonium, allowing a compact storage ring without electric focusing of muons. J-PARC E34 is expected to have different systematic uncertainties, and

therefore it would provide a good cross-check of the BNL E821 result. It is noted that the electron ($g_e - 2$) has also about 2σ deviation from the SM prediction, but an opposite sign [8].

2.2. Status of the neutron lifetime puzzle

The neutron decays due to the weak interaction process $n \rightarrow p e^- \bar{\nu}$. Given its importance in particle physics and cosmology, the neutron lifetime τ_n has been measured by more than 20 experiments since the 1950's. There is now a persistent disagreement between the two classes of methods to measure the lifetime, the so called “beam” and “bottle” methods [9].

In the “beam” method [10], one counts the rate of appearance \dot{N} of protons in a neutron beam within a fiducial volume containing N neutrons. One gets the neutron lifetime from the relation $\dot{N} = N/\tau_n$. This method requires an absolute measurement of the neutron flux to determine N and also requires to know the efficiency of the detector counting the protons. The “beam” average is

$$\tau_n^{\text{beam}} = 888.0 \pm 2.0 \text{ s.} \quad (10)$$

In the “bottle” method, one uses trapped ultracold neutrons (UCNs). UCNs are neutrons with kinetic energy lower than about 200 neV. In this extremely low energy range, the neutrons are reflected off material surfaces at any angle of incidence (in contrast with cold neutrons which are reflected only at grazing incidence from the surface). Therefore UCNs can be trapped in evacuated material containers called “bottles”. The method of the experiment consists in loading a bottle with UCNs and counting how many remain after some time t . By repeating the measurement for various times t , the storage time τ_n^{bottle} is extracted from a fit of the storage curve $N(t) = N_0 e^{-t/\tau_n^{\text{bottle}}}$. The experiments with UCNs are consistently reporting a lifetime shorter than the “beam” average. In UCN experiments one has to control all the neutron losses in the bottle which come in addition to the beta decay. In particular a correction for the losses due to wall collisions has to be applied, it was about 15 s in the most recent experiment of this type [11]. It was tempting to attribute the lifetime discrepancy to unaccounted errors in the wall losses correction. However, in the more recent experiments [12, 13], UCNs are contained in magnetic bottles (the magnetic potential barrier is 60 neV/T for neutrons) and never hit any material surfaces. These magnetic storage experiments confirmed the results with material traps, which makes the neutron lifetime puzzle more puzzling. The “bottle” average is now

$$\tau_n^{\text{bottle}} = 879.4 \pm 0.6 \text{ s.} \quad (11)$$

The discrepancy is as large as $\tau_n^{\text{beam}} - \tau_n^{\text{bottle}} = 8.6 \pm 2.1 \text{ s}$ (4 standard deviations).

Interestingly, the “bottle” method measures the total decay rate of the neutron whereas the “beam” method measures the partial decay to protons. The discrepancy could be explained by an invisible decay channel for the neutron with a branching ratio of about 1%. However this possibility has been ruled out [14, 15] by comparing the results with the theoretical predictions. In the Standard Model, τ_n can be calculated from the masses of the particles, the Fermi constant G_F (accurately determined from the muon lifetime), the CKM matrix element V_{ud} , and $\lambda = g_A/g_V$ the ratio of the axial to vector coupling of the nucleon. The value of λ could in principle be calculated from QCD, but the precision of lattice calculations of order 1% is presently insufficient. Instead, λ is extracted from neutron decay correlation coefficients. It turns out that the SM prediction [15]

$$\tau_n^{\text{SM}} = 879.4 \pm 1.0 \text{ s} \quad (12)$$

agrees very well with the “bottle” average and is incompatible with the “beam” average. This rules out the invisible channel hypothesis, which predicts the contrary.

The situation with the neutron lifetime puzzle is serious. It must be settled experimentally, in particular with an improved beam experiment measuring the proton rate [16], and with a new beam experiment measuring the electron rate at J-PARC [17].

3. Lepton flavor violating processes with muons

3.1. Physics motivation of charged lepton flavour violation (CLFV)

In the minimal SM, neutrinos are massless and lepton flavor is conserved separately for each generation. However it has been known and confirmed that neutrinos are not massless and mixed by the observation of neutrino oscillation. Therefore lepton flavor is not conserved in the SM. The SM contribution to the CLFV rates, such as $\mu^+ \rightarrow e^+ \gamma$ can be estimated by [18]

$$B(\mu^+ \rightarrow e^+ \gamma) = \frac{3\alpha}{32\pi} \left| \sum_{\ell=1}^3 (V_{\text{MNS}})_{\mu\ell}^* (V_{\text{MNS}})_{e\ell} \frac{m_{\nu_\ell}^2}{M_W^2} \right|^2 \sim \mathcal{O}(10^{-54}) \quad (13)$$

where V_{MNS} is the PMNS lepton mixing matrix element in the SM. m_{ν_ℓ} ($\ell = 1, 3$) and M_W is the neutrino masses and the W boson mass respectively. The SM contribution is thus very small, providing a large window of experimental searches for new physics beyond the SM (BSM) without SM backgrounds.

The sensitivity of CLFV can be estimated, for instance, by using an effective field theory (EFT) approach. The effective Lagrangian (\mathcal{L}) is given by

$$\mathcal{L} = \mathcal{L}_{\text{SM}} + \sum_{d>4} \frac{C^{(d)}}{\Lambda^{d-4}} \mathcal{O}^{(d)}, \quad (14)$$

where \mathcal{L}_{SM} is the Standard Model Lagrangian, $C^{(d)}$ is the coupling constant, Λ is the energy scale of new physics, $\mathcal{O}^{(d)}$ is an operator of dimension d . For instance, the current upper bound of $B(\mu^+ \rightarrow e^+ \gamma) < 4.2 \times 10^{-13}$ at 90% C.L. could yield $\Lambda \sim \mathcal{O}(10^4)$ TeV for the coupling constant of $C \sim \mathcal{O}(1)$ [19, 20]. Its sensitivity to energy scale of BSM has already reached to significantly high, well above that the current and planned accelerators can directly reach. Furthermore, as mentioned later, the currently-planned experiments are expecting sensitivity improvements of a factor of more than 10,000 from the current limits. With the dimension-six operators, the rate is proportional to $1/\Lambda^4$, suggesting that the energy reach of new physics can be extended by additional factor of ten, to $\mathcal{O}(10^5)$ TeV in the future. Also there are many theoretical models to predict sizable CLFV rates, some of which are just below the current experimental limits. They are, for example, the models with neutral heavy leptons, extra-dimension, Z' , leptoquark, supersymmetry and so on.

3.2. Phenomenology of CLFV

The most sensitive studies of CLFV are made by experiments to search for $\mu \rightarrow e$ transitions by utilizing highly intense muon beams. They are $\mu^+ \rightarrow e^+ \gamma$, $\mu^+ \rightarrow e^+ e^- e^+$, and $\mu^- \rightarrow e^-$ conversion in a muonic atom.

$\mu^+ \rightarrow e^+ \gamma$ decay: The effective Lagrangian for the $\mu^+ \rightarrow e^+ \gamma$ amplitude is given by

$$\mathcal{L}_{\mu \rightarrow e \gamma} = -\frac{4G_F}{\sqrt{2}} [m_\mu A_R \bar{\mu}_R \sigma^{\mu\nu} e_L F_{\mu\nu} + m_\mu A_L \bar{\mu}_L \sigma^{\mu\nu} e_R F_{\mu\nu} + \text{h.c.}], \quad (15)$$

where A_R and A_L are coupling constants that correspond to the processes of $\mu^+ \rightarrow e_R^+ \gamma$ and $\mu^+ \rightarrow e_L^+ \gamma$, respectively. $\mu_{R(L)}$ is a right-handed (left-handed) positive muon, and $e_{R(L)}$ is a right-handed (left-handed) positron, G_F is the Fermi coupling constant and $F_{\mu\nu}$ is the electromagnetic tensor. This Lagrangian presents a dipole-type interaction with photons, but changing lepton flavor. Then the branching fraction (\mathcal{B}) is given by

$$\mathcal{B}(\mu^+ \rightarrow e^+ \gamma) = \frac{\Gamma(\mu^+ \rightarrow e^+ \gamma)}{\Gamma(\mu^+ \rightarrow e^+ \nu)} = 384\pi^2 (|A_R|^2 + |A_L|^2). \quad (16)$$

The event signature of $\mu^+ \rightarrow e^+ \gamma$ decay at rest is a positron and a photon are moving back-to-back in coincidence with their energies equal to half that of the muon mass ($m_\mu/2 = 52.8$ MeV). The searches in the past were made by using positive muons at rest to fully utilize its kinematics. Negative muons have not been used because they are captured by a nucleus when they are stopped in a material. There are two major backgrounds to the search for $\mu^+ \rightarrow e^+ \gamma$ decay. One of them is a physics background from radiative muon decay, $\mu^+ \rightarrow e^+ \nu \bar{\nu} \gamma$ when e^+ and photon are emitted back-to-back with the two neutrinos carrying off a small amount of energy. The other background is an accidental coincidence of a positron in a normal muon decay accompanied by a high energy photon. Possible sources of the high energy photon would be either $\mu^+ \rightarrow e^+ \nu \bar{\nu} \gamma$ decay, annihilation-in-flight or external bremsstrahlung of e^+ s from a normal muon decay. To reduce accidental background events, an instantaneous rate of incident muons should be kept low, and thus a continuous muon beam should be utilized.

$\mu^+ \rightarrow e^+ e^- e^+$ decay: The $\mu^+ \rightarrow e^+ e^- e^+$ decay could have not only the dipole-type photonic contribution but also four-fermion contributions. The effective Lagrangian for $\mu^+ \rightarrow e^+ e^- e^+$ can have two dipole operators and six four-fermion operators with different combinations of lepton chirality. If only the dipole-type photonic diagrams contribute to $\mu^+ \rightarrow e^+ e^- e^+$ decay, a model-independent relation between the two branching ratios can be derived, $\mathcal{B}(\mu^+ \rightarrow e^+ e^- e^+)/\mathcal{B}(\mu^+ \rightarrow e^+ \gamma) \simeq 0.006$ [2].

The event signature of $\mu^+ \rightarrow e^+ e^- e^+$ decay is kinematically well constrained, since all particles in the final state are detectable with high precision. Muon decay at rest has been used in all past experiments. In this case, the conservation of momentum sum ($|\sum_i \vec{p}_i| = 0$) and energy sum ($\sum_i E_i = m_\mu$) could be effectively used together with the timing coincidence between two e^+ s and one e^- , where \vec{p}_i and E_i ($i = 1, 3$) are respectively the momentum and energy of each of the e^+ s. One of the physics background processes is the allowed muon decay $\mu^+ \rightarrow e^+ \nu \bar{\nu} e^+ e^-$ ($\mathcal{B} = (3.4 \pm 0.4) \times 10^{-5}$), which becomes a serious background when ν_e and $\bar{\nu}_\mu$ have very small energies. The other background is an accidental coincidence of an e^+ from normal muon decay with an uncorrelated $e^+ e^-$ pair, where a $e^+ e^-$ pair could be produced either from Bhabha scattering of e^+ , or from the external conversion of the photon in $\mu^+ \rightarrow e^+ \nu_e \bar{\nu}_\mu \gamma$ decay. As has been discussed for the $\mu^+ \rightarrow e^+ \gamma$ search, to reduce accidental background events, a continuous muon beam should be utilized.

$\mu^- \rightarrow e^-$ conversion: The third important $\mu \rightarrow e$ transition process is neutrino-less conversion of a negative muon to an electron in the field of a nucleus of a muonic atom. When a negative muon is stopped in some material, it is trapped by an atom, and a muonic atom is formed. After it cascades down energy levels in the muonic atom, the muon is bound in its 1s ground state. The fate of the muon is then either decay in orbit ($\mu^- N(A, Z) \rightarrow e^- \nu_\mu \bar{\nu}_e N(A, Z)$) or nuclear muon capture, namely, $\mu^- N(A, Z) \rightarrow \nu_\mu N(A, Z-1)$, for a nucleus $N(A, Z)$ of mass number A and atomic number Z . However, in the context of BSM, the CLFV process of neutrino-less muon capture, such as

$$\mu^- N(A, Z) \rightarrow e^- N(A, Z), \quad (17)$$

is also expected. This process is called $\mu^- \rightarrow e^-$ conversion in a muonic atom. The final state of the nucleus $N(A, Z)$ could be either the ground state or one of the excited states. In general, the transition to the ground state, which is called coherent conversion, is dominant. The rate of the coherent capture over non-coherent capture is enhanced by a factor approximately equal to the number of nucleons in the nucleus. The conversion rate of $\mu^- \rightarrow e^-$ conversion is defined as $\text{CR}(\mu^- N \rightarrow e^- N) \equiv \Gamma(\mu^- N \rightarrow e^- N)/\Gamma(\mu^- N \rightarrow \text{all})$, where Γ is the rate. The time distribution of $\mu^- \rightarrow e^-$ conversion follows a lifetime of a muonic atom, which depends on a nucleus.

The event signature of $\mu^- \rightarrow e^-$ conversion in a muonic atom is a mono-energetic single electron emitted from the conversion with an energy ($E_{\mu e}$) of $E_{\mu e} = m_\mu - B_\mu - E_{\text{recoil}}$, where m_μ is

the muon mass, and B_μ is the binding energy of the $1s$ muonic atom. E_{recoil} is the nuclear recoil energy. Since B_μ varies for various nuclei, $E_{\mu e}$ could be different. For instance, $E_{\mu e} = 104.9$ MeV for aluminium (Al), $E_{\mu e} = 104.3$ MeV for titanium (Ti), and $E_{\mu e} = 94.9$ MeV for lead (Pb). The potential background sources for $\mu^- \rightarrow e^-$ conversion can be grouped into three. The first group is intrinsic physics backgrounds which come from muons stopped in the muon-stopping target, such as electrons from muon decays in orbit and radiative muon capture. The second is beam-related backgrounds which are caused by beam particles in a muon beam. To eliminate beam-related backgrounds, a pulsed proton beam is used and the measurement will be made between the beam pulses. The third is backgrounds coming from cosmic-ray muons, fake tracking events, and so on.

The effective Lagrangian of $\mu^- \rightarrow e^-$ conversion can be expressed by dipole, scalar, vector, pseudo-scalar, axial-vector and tensor interactions. Among these effective interactions, the dipole, scalar and vector operators contribute to the spin independent (SI) $\mu^- \rightarrow e^-$ conversion processes, whereas the axial, tensor and pseudo-scalar operators contribute to the spin dependent (SD) $\mu^- \rightarrow e^-$ conversion [21]. The SI process is a coherent process which does benefit from nucleon-number-squared enhancement, but the SD process does not. The rates of the SI processes for various nuclei were calculated, showing the dependence of atomic charge (Z) could be used to discriminate different type of effective interactions [22, 23].

3.3. Current limits and future prospects

$\mu^+ \rightarrow e^+ \gamma$ decay: The present experimental upper limit is $\mathcal{B}(\mu^+ \rightarrow e^+ \gamma) < 4.2 \times 10^{-13}$ at 90% CL [24], which was obtained by the MEG experiment at PSI from data collected from 2009–2013. The MEG used a monochromatic beam (of 28 MeV/ c) of surface positive muons, which are produced by pion decays at rest at the surface of a proton target. The MEG detector consisted of drift chambers to detect e^+ s and a scintillation detector of 900 l of liquid xenon to measure photons. The detectors were placed inside a superconducting solenoid with a graded magnetic field along the beam axis.

The MEG II experiment [25] has a better e^+ spectrometer with a new cylindrical drift chamber and pixelated precision timing counter, and a liquid xenon photon detector read out by new silicon photomultipliers (at the central region) and photomultipliers (at the forward/backward regions). Fine segmentation of silicon photomultipliers would improve the position and angular resolution of photon detection. Additional detector to eliminate $\mu^+ \rightarrow e^+ \nu \bar{\nu} \gamma$ backgrounds is newly introduced. The detector construction is complete. Each of the upgraded detectors is expected to provide resolutions roughly a factor of two better than MEG, allowing them to use the full muon beam intensity at PSI. The MEG II aims to achieve a factor of ten improvement, reaching 6×10^{-14} .

$\mu^+ \rightarrow e^+ e^- e^+$ decay: The current experimental limit of $\mathcal{B}(\mu^+ \rightarrow e^+ e^- e^+) < 1 \times 10^{-12}$ at 90% CL was obtained by the SINDRUM experiment from data collected from 1983–1986 [26]. This limit was obtained by assuming the constant matrix element of the $\mu^+ \rightarrow e^+ e^- e^+$ decay.

The Mu3e experiment [27] is aiming at $\mathcal{B}(\mu^+ \rightarrow e^+ e^- e^+) < 5 \times 10^{-15}$ at 90% CL in its first stage at the existing $\pi E5$ beamline at PSI. The Mu3e detector consists of ultra-thin, monolithic, silicon pixel tracking detectors based on the HV-MAPS technology, and a scintillating fiber system to measure timing in a sub-nanosecond resolution. All the detectors are located in a superconducting solenoid of 1 T magnetic field. After three years of operation, Mu3e Phase-I will reach the aimed sensitivity. This sensitivity is limited by the muon rate at the $\pi E5$ at PSI. At PSI, a new High Intensity Muon Beamline, HiMB, has been investigated. It would provide 1.3×10^{10} surface μ^+ s/s. Mu3e Phase-II, the second stage of the experiment, will utilize a highly intense

muon beam at the HiMB, aiming at another factor of ten improvement, to $\mathcal{B}(\mu^+ \rightarrow e^+ e^- e^+) < 1 \times 10^{-16}$ at 90% CL.

$\mu^- \rightarrow e^-$ conversion: The past experimental searches for $\mu^- \rightarrow e^-$ conversion were made with five different materials of muon stopping target, such as sulphur ($Z = 16$), titanium ($Z = 22$), copper ($Z = 39$), gold ($Z = 79$), and lead ($Z = 82$). Among them, the best limit is $\text{CR}(\mu^- \text{Au} \rightarrow e^- \text{Au}) < 7 \times 10^{-13}$ at 90% CL, which was obtained by the SINDRUM-II experiment, from data collected from 2000 [28].

There are two new experiments to search for $\mu^- \rightarrow e^-$ conversion under preparation; one is the Mu2e experiment in the US and the other is the COMET experiment in Japan.

The Mu2e experiment [29] at Fermilab is aiming at $\text{CR}(\mu^- \text{Al} \rightarrow e^- \text{Al}) < 8 \times 10^{-17}$ at 90% CL with an aluminium target for 690 days of operation. 8 GeV protons with 8 kW from the Fermilab Booster with 1.7 μs intervals are delivered to a proton target of tungsten placed inside the high magnetic-field solenoids. The muons from pion decays are transported through two 90° curved solenoids in the opposite bending direction, forming a “S” shape, where momentum and charge of muons are selected by collimators located after the first 90° bend, and the second 90° bend brings the muons to the center of the beamline. Then the muons are delivered to a muon stopping target, which is placed in a graded magnetic field. The detector consists of straw tube drift chambers and an electron calorimeter of pure CsI crystals in a constant magnetic field region. The whole detector is covered by the scintillator based cosmic veto system. The Mu2e experiment can be upgraded to Mu2e-II [30], to take advantage of the high intensity proton beam available at the PIP-II project in the future. The PIP-II linac, under consideration at Fermilab, would provide 1.6 MW of 0.8 GeV protons. The Mu2e-II will utilize 100 kW of protons from PIP-II to increase its sensitivity by a factor of ten or more.

The COMET experiment has taken a two-staged approach. The COMET Phase-I [31, 32], the first stage of the experiment, is aiming at $\text{CR}(\mu^- \text{Al} \rightarrow e^- \text{Al}) < 7 \times 10^{-15}$ at 90% C.L. for 150 days of operation. 8 GeV protons with 3.2 kW from the J-PARC main ring will be delivered to a proton target made of graphite inside the 5 T pion capture solenoid. The muon transport consists of a 90° curved solenoids, together with dipole coils installed inside the solenoids, providing momentum and charged selection by changing a dipole magnetic field. The detector to search for $\mu^- \rightarrow e^-$ conversion in COMET Phase-I is a cylindrical drift chamber. And low-mass straw tube drift chambers and a LYSO crystal calorimeter, which are the COMET Phase-II detector, will be used for beam measurement in COMET Phase-I. The COMET Phase-I will be extended to COMET Phase-II [33], the second stage, whose sensitivity is $\text{CR}(\mu^- \text{Al} \rightarrow e^- \text{Al}) < 6 \times 10^{-17}$ at 90% CL with 56 kW proton beam power for 230 days of operation. The proton target for Phase-II is made of tungsten. The muon transport at Phase-II consists of two 90° curved solenoids with the same bending direction, forming a “C” shape, where continuous 180° bend will be fully utilized to make twice better momentum and charge separation than single 90° bend. The electron transport, which is installed between the muon target and the detector, has a 180° curved solenoid to select 105 MeV/c electrons and eliminate positive-charged particles (such as protons from muon capture) and low energy electrons from normal muon decays. This curved electron transport also eliminates a direct sight from the detector to the muon target to remove neutron and γ -ray backgrounds, which would otherwise cause serious high detector rates. Recently, further improvements of sensitivity by one order of magnitude, yielding a sensitivity of $\mathcal{O}(10^{-18})$, from refinements to the experimental design and operation are being considered [34].

High intensity muon beam sources: Expected significant improvements in high intensity frontier with muons would benefit from the planned muon sources with their intensities of more than $10^{10} \mu^\pm/\text{s}$. At PSI, the HiMB with 1.3×10^{10} surface muons/second is being considered with new capture and beamline solenoids at the Target M station. The Mu2e and COMET muon beams

could produce 10^{10} – 10^{11} μ^- /s with 8 GeV proton beams of 8 kW and 56 kW beam power, respectively. These high intensity muon beams can be realized with a 5 T pion capture solenoid system surrounding a proton target, followed by a curved solenoid magnet which provides a charge and momentum-selected muon beam to an experiment. Furthermore, the muon beam system adopted in Mu2e and COMET was originally proposed by Lobashev and Dzhilkibaev in 1989 [35]. The first experimental demonstration of the feasibility of the method was achieved at the Research Center of Nuclear Physics, Osaka University in 2011 [36]. In the long term future, a cooled muon beam of smaller beam emittance can be considered to make better CLFV measurements. The cooled muon beams can be made based on some novel techniques of phase rotation and ionizing cooling, which have been developed in the R&D of a muon collider and a neutrino factory. The PRISM concept [37] utilizing phase rotation of muons in a muon storage ring was considered and tested in Japan. The development of a new high-intensity muon beam of better emittance would be a key to make further significant progress in this field.

4. The neutron electric dipole moment

4.1. n EDM as a probe of new CP -violating physics

The electric dipole moment d of a fermion f , from the point of view of relativistic field theory, is the coupling constant of the CP violating interaction with the electromagnetic field $F_{\mu\nu}$:

$$\mathcal{L}_{\text{EDM}} = -\frac{id}{2} \bar{f}_L \sigma^{\mu\nu} f_R F_{\mu\nu} + \text{h.c.} \quad (18)$$

where f_L and f_R are the left and right chirality components of the fermion. This effective non-renormalizable interaction is generated by virtual effects, as depicted generically in Figure 1(a). In fact the imaginary part of the diagram generate the EDM whereas the real part generate the anomalous magnetic moment. A specific loop diagram involving a scalar boson of mass M and with a complex coupling g to the fermion is shown in Figure 1(b). It generates an EDM of $d \approx e\hbar c \text{Im}(g^2)/(4\pi)^2 m_f/M^2$. This pedagogical example can be used to estimate the EDM of the first generation fermions – say the d quark ($m_f = 5$ MeV) – induced by a boson at the TeV scale ($M \approx 1$ TeV and $\text{Im}(g^2)/(4\pi) \approx 10^{-2}$). We get $d \approx 10^{-25}$ e cm, a value in the reach of neutron¹ EDM experiments given that the current upper limit is [38]

$$|d_n| < 3 \times 10^{-26} \text{ e cm (90\% C.L.)}. \quad (19)$$

The Standard Model contains two sources of CP violation: the complex phase in the CKM matrix and the strong phase θ_{QCD} . Due to the peculiar flavour structure of the electroweak theory, the neutron EDM induced by the CKM phase is undetectably small: $d_n \sim 10^{-32}$ e cm. This is because only diagrams involving all three generations of quarks in the loops can contribute to the imaginary part of the interaction Figure 1(a). A nonzero strong phase, on the contrary, would induce a large neutron EDM. The limit (19) translates to the bound $|\theta_{\text{QCD}}| < 10^{-10}$, a severe fine-tuning known as the *strong CP problem*. It is believed that physics beyond the Standard Model is at play to set this phase to zero with an Axion mechanism.

Then, EDMs are sensitive probes of CP violation effects beyond the Standard Model with practically zero background. As an illustrative example let us consider the search for CP -violating couplings of the Higgs boson h to fermions. The Higgs couplings are generically parameterized by the following lagrangian

$$\mathcal{L}_h = -\frac{y_f}{\sqrt{2}} (\kappa_f \bar{f} f h + i\tilde{\kappa}_f \bar{f} \gamma_5 f h), \quad (20)$$

¹The EDM of the light quarks generate a neutron EDM with coefficients of order unity.

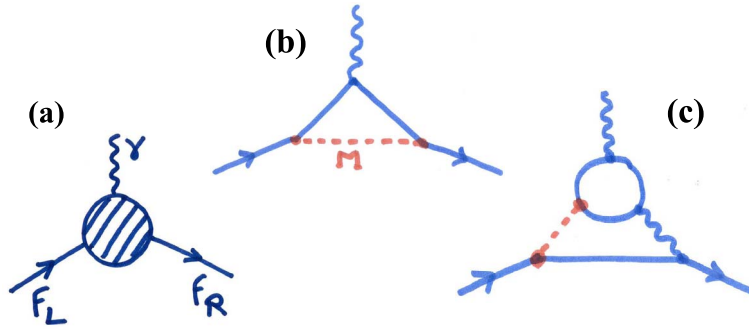


Figure 1. (a) Feynman diagram corresponding to the EDM coupling (18). (b) Example of a one-loop diagram contributing to the fermion EDM. (c) Two-loop Barr-Zee diagram contributing to the fermion EDM.

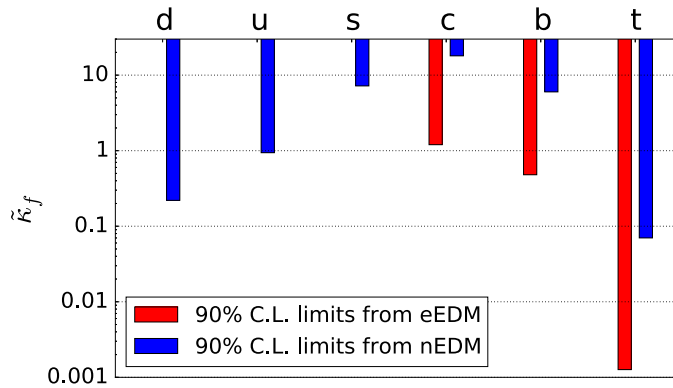


Figure 2. Current limits on the CP -violating couplings of the Higgs boson for the six quark flavours derived from the electron EDM (red bars) and from the neutron EDM (blue bars), adapted from [39–41].

where y_f is the Yukawa coupling of the fermion f , κ_f and $\tilde{\kappa}_f$ are the CP -conserving and CP -violating coupling constants. The Standard Model predicts $\kappa_f = 1$ and $\tilde{\kappa}_f = 0$. This coupling generates EDMs through the two-loops diagram shown in Figure 1(c). The limits on the CP -violating couplings to the quarks derived from the neutron and electron EDM bounds are shown in Figure 2. This plot illustrates the complementarity of EDM searches: the electron EDM is more sensitive to $\tilde{\kappa}$ of the heavy quarks while the neutron EDM is more sensitive to $\tilde{\kappa}$ of the light quarks. It also illustrates the great sensitivity of EDM searches: fundamental CP -violating couplings of order unity, relative to CP -conserving couplings, are already excluded except for the s quark. Next generations of EDM experiments will push these limits down by an order of magnitude, or perhaps discover a signal induced by small CP -violation in the Higgs sector.

Extra CP violation is a generic feature of models extending the SM, which inevitably come with additional complex (therefore CP -violating) free parameters. Also, a new source of CP violation is required to explain the matter-antimatter asymmetry. Indeed CP violation is one of Sakharov's necessary condition to generate dynamically the baryon asymmetry in the early Universe. EDM limits are highly relevant for the *Electroweak baryogenesis* scenario. In this class of models, baryogenesis occurred at the electroweak phase transition epoch of the Universe, at a temperature of about 100 GeV. See [42] for a recent discussion on the subject. For baryogenesis

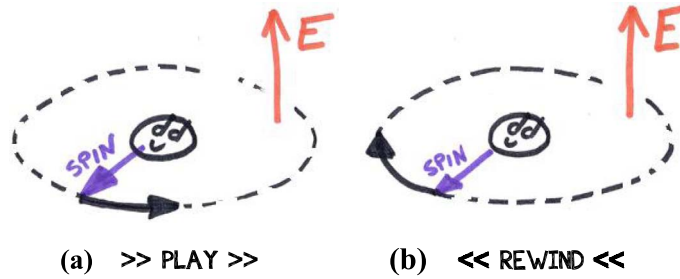


Figure 3. (a) Evolution in an electric field of a particle spin with a non-zero – negative in this case – EDM. (b) Time-reversed version of the evolution (a). The fact that (a) and (b) are different constitutes a violation of time reversal symmetry.

to work, new CP -violating interactions must have been active at this temperature, therefore the mass of the new particles could not be much heavier than 1 TeV and the CP -violating interaction they mediate should be sufficiently strong. The models therefore also predict sizable EDMs and the future EDM experiments will either discover a nonzero EDM or exclude most of electroweak baryogenesis models.

4.2. State of the art of the experiments and future prospects

In the non-relativistic limit the lagrangian density (18) reduces to the following Hamiltonian:

$$\hat{H} = -d\hat{\sigma} \cdot \vec{E}, \quad (21)$$

where $\hat{\sigma}$ are the Pauli matrices acting on the fermion's spin states and \vec{E} is the applied external electric field. The electric dipole moment quantifies the coupling between the spin and the electric field, in the same way that the magnetic moment μ quantifies the coupling between the spin and the magnetic field. The time evolution is shown in Figure 3: the spin precesses around the field at an angular frequency given by $\hbar\omega = 2dE$. As Figure 3(b) shows, the existence of a non-zero EDM would constitute a violation of time reversal symmetry. It is consistent with the fact that the lagrangian (18) violates the CP symmetry, because T -violation is equivalent to CP -violation in any local relativistic quantum field theory.

The basic idea to measure the neutron EDM is to use polarized neutrons and measure precisely the spin precession frequency f in parallel or antiparallel magnetic and electric fields:

$$f = \frac{\mu}{\pi\hbar}B_0 \pm \frac{d}{\pi\hbar}E. \quad (22)$$

The EDM term can be separated from the much larger magnetic term by taking the difference of the frequency measured in parallel and antiparallel configurations. The EDM term, if it exists, is extremely small ($dE/\pi\hbar \approx 10^{-7}$ Hz for $d = 10^{-26}$ e cm and $E = 15$ kV/cm) compared to the magnetic term (typically, $f = 29$ Hz for $B_0 = 1$ μ T).

To detect such a minuscule coupling, one needs (i) a long interaction time of the neutrons with the electric field, (ii) a high flux of neutrons and (iii) a precise control of the magnetic field. In the first experiment [43] Smith, Purcell and Ramsey used a beam of thermal neutrons passing in the electric field during $T \approx 1$ ms. In the 1980s, the precession time could be greatly increased by using *ultracold neutrons* (UCNs). These are neutrons with a kinetic energy smaller than the neutron optical potential of solid materials, typically 100 neV. These neutrons can therefore be stored in material traps because they undergo total reflection upon collision with the walls of the trap. In the best previous measurement [38] performed at ILL in the period 1998–2002, UCNs were stored in a chamber permeated by a weak magnetic field and a strong electric field during

Table 1. List of active ongoing nEDM projects [45]

Project	Location	Concept	Reference
nEDM@SNS	Oak Ridge spallation source	UCN in superfluid helium with ^3He comagnetometer	[46]
n2EDM	PSI spallation source	UCN large double chamber with ^{199}Hg comagnetometer	[47]
nEDM@LANL	Los Alamos spallation source	UCN double chamber with ^{199}Hg comagnetometer	[48]
panEDM	ILL reactor Grenoble	UCN double chamber	[52]
TUCAN	TRIUMF spallation source	UCN double chamber with ^{199}Hg or ^{129}Xe comagnetometer	[49]
PNPI nEDM	ILL - PNPI	UCN double chamber	[50]
beam nEDM	ESS spallation source	Pulsed cold neutron beam	[51]

$T \approx 100$ s. Although the systematic error is also a big concern, this measurement was limited by the statistical error and thus by the intensity of the ILL/PF2 UCN source. New higher intensity UCN sources are now coming online at several major neutron factories worldwide, which are exploited by several nEDM projects. In particular, the nEDM experiment has collected data [44] in 2015–2016 at the PSI UCN source, which will result in a marginally improved measurement of the neutron EDM (the analysis is still ongoing at the time of writing). Other ongoing nEDM projects [45–51] are listed in Table 1, they are all at a different stage of readiness and they aim at an improvement in sensitivity by a factor 10 to 100 compared to the previous measurement [38] in the next decade. These projects to measure the neutron EDM are an important part of a global search for fundamental EDMs. A variety of programmes with different systems are being pursued [45], with free neutrons, diamagnetic atoms, paramagnetic systems, charged particles (muons, protons, deuterons) in storage rings and heavy unstable particles (lepton τ , hyperons and charmed baryons) at particle colliders.

5. Conclusion

This precision physics programs of muons and neutrons are presently very productive and active, even after their long history of over 80 years. There are many new experiments being under preparation or planned. The anomalies of the muon ($g_\mu - 2$) and the neutron lifetime would be hopefully resolved in a coming few years to address new physics. Over next years, currently planned experiments searching for CLFV $\mu^- \rightarrow e^-$ transitions would improve their sensitivities by a factor of 10 to more than 10,000. The experiments to search for the neutron EDM would improve their sensitivities by a factor of 10 to 100 over the current limit.

In summary, the physics with muons and neutrons, in particular the muon CLFV and the neutron EDM, provide an unique discovery potential to new physics beyond the SM. They are expected to play a leading role in the search for BSM, and offer extraordinary opportunities for exploring new phenomena which would otherwise be directly inaccessible at future high-energy colliders.

References

- [1] D. Dubbers, M. G. Schmidt, “The neutron and its role in cosmology and particle physics”, *Rev. Mod. Phys.* **83** (2011), no. 4, p. 1111-1171.
- [2] Y. Kuno, Y. Okada, “Muon decay and physics beyond the standard model”, *Rev. Mod. Phys.* **73** (2001), p. 151-202.

- [3] L. Calibbi, G. Signorelli, “Charged lepton flavour violation: An experimental and theoretical introduction”, *Riv. Nuovo Cimento* **41** (2018), no. 2, p. 71-174.
- [4] A. Keshavarzi, D. Nomura, T. Teubner, “Muon g-2 and (MZ2): a new data-based analysis”, *Phys. Rev. D* **97** (2018), article ID 114025.
- [5] G. W. Bennett *et al.* (Muon g-2 collaboration), “Final report of the E821 muon anomalous magnetic moment measurement at BNL”, *Phys. Rev. D* **73** (2006), article ID 072003.
- [6] J. Grange *et al.* (Muon g-2 Collaboration), “Muon (g-2) Technical Design Report”, 2019, preprint, <https://arxiv.org/abs/1501.06858>.
- [7] M. Abe *et al.* (J-PARC muon/edm collaboration), “A new approach for measuring the muon anomalous magnetic moment and electric dipole moment”, *Progr. Theoret. Exp. Progress* **2019** (2019), article ID 053C02.
- [8] D. Hanneke, S. F. Hoogerheide, G. Gabrielse, “Cavity control of a single-electron quantum cyclotron: measuring the electron magnetic moment”, *Phys. Rev. A* **83** (2011), article ID 052122.
- [9] F. E. Wietfeldt, “Measurements of the neutron lifetime”, *Atoms* **6** (2018), no. 4, article ID 70.
- [10] A. T. Yue, M. S. Dewey, D. M. Gilliam, G. L. Greene, A. B. Laptev, J. S. Nico, W. M. Snow, F. E. Wietfeldt, “Improved determination of the neutron lifetime”, *Phys. Rev. Lett.* **111** (2013), no. 22, article ID 222501.
- [11] A. P. Serebrov *et al.*, “Neutron lifetime measurements with a large gravitational trap for ultracold neutrons”, *Phys. Rev. C* **97** (2018), no. 5, article ID 055503.
- [12] V. F. Ezhov *et al.*, “Measurement of the neutron lifetime with ultra-cold neutrons stored in a magneto-gravitational trap”, *JETP Lett.* **107** (2018), no. 11, p. 671-675.
- [13] R. W. Pattie Jr. *et al.*, “Measurement of the neutron lifetime using a magneto-gravitational trap and in situ detection”, *Science* **360** (2018), no. 6389, p. 627-632.
- [14] A. Czarnecki, W. J. Marciano, A. Sirlin, “Neutron lifetime and axial coupling connection”, *Phys. Rev. Lett.* **120** (2018), no. 20, article ID 202002.
- [15] D. Dubbers, H. Saul, B. Märkisch, T. Soldner, H. Abele, “Exotic decay channels are not the cause of the neutron lifetime anomaly”, *Phys. Lett. B* **791** (2019), p. 6-10.
- [16] F. E. Wietfeldt, G. Darius, M. S. Dewey, N. Fomin, G. L. Greene, J. Mulholland, W. M. Snow, A. T. Yue, “A path to a 0.1 s neutron lifetime measurement using the beam method”, *Phys. Proc.* **51** (2014), p. 54-58.
- [17] N. Nagakura *et al.*, “Precise neutron lifetime experiment using pulsed neutron beams at J-PARC”, *PoS INPC 2016* (2017), article ID 191.
- [18] S. T. Petcov, “The processes $\mu \rightarrow e \gamma$, $\mu \rightarrow e \text{ anti-}e$, Neutrino' \rightarrow Neutrino gamma in the Weinberg–Salam model with neutrino mixing”, *Sov. J. Nucl. Phys.* **25** (1977), p. 340.
- [19] F. Feruglio, P. Paradisi, A. Pattori, “Lepton flavour violation in composite Higgs models”, *Eur. Phys. J. C* **75** (2015), article ID 579.
- [20] G. M. Pruna, A. Singer, “The $\mu \rightarrow e \gamma$ decay in a systematic effective field theory approach with dimension 6 operators”, *JHEP* **1410** (2014), article ID 014.
- [21] V. Cirigliano, S. Davidson, Y. Kuno, “Spin-dependent $\mu \rightarrow e$ conversion”, *Phys. Lett. B* **771** (2017), p. 242-246.
- [22] R. Kitano, M. Koike, Y. Okada, “Detailed calculation of lepton flavor violating muon-electron conversion rate for various nuclei”, *Phys. Rev. D* **66** (2002), article ID 096002, [Erratum *Phys. Rev. D* **76** (2017), 059902].
- [23] V. Cirigliano, R. Kitano, Y. Okada, P. Tuzon, “Model discriminating power of $\mu \rightarrow e$ conversion in nuclei”, *Phys. Rev. D* **80** (2009), article ID 013002.
- [24] A. Baldini *et al.* (MEG Collaboration), “Search for the lepton flavour violating decay $\mu^+ \rightarrow e^+ \gamma$ with the full dataset of the MEG experiment”, *Eur. Phys. J. C* **76** (2016), article ID 434.
- [25] A. Baldini *et al.* (MEG II Collaboration), “The design of the MEG II experiment”, *Eur. Phys. J. C* **78** (2018), article ID 380.
- [26] U. Bellgardt *et al.* (SINDRUM Collaboration), “Search for the decay $\mu^+ \rightarrow e^+ e^+ e^-$ ”, *Nucl. Phys. B* **299** (1988), no. 1, p. 1-6.
- [27] A. Blondel *et al.* (Mu3e Collaboration), “Research Proposal for an Experiment to Search for the Decay $\mu \rightarrow eee$ ”, 2013, preprint, <https://arxiv.org/abs/1309.7679>.
- [28] W. Bertl *et al.* (SINDRUM-II Collaboration), “A search for muon to electron conversion in muonic gold”, *Eur. Phys. J. C* **47** (2006), article ID 337.
- [29] L. Bartoszek *et al.* (Mu2e Collaboration), “Mu2e Technical Design Report”, 2015, preprint, <https://arxiv.org/abs/1501.05241>.
- [30] F. Abusalma *et al.* (Mu2e-II Collaboration), “Expression of Interest for Evolution of the Mu2e Experiment”, 2018, preprint, <https://arxiv.org/abs/1802.02599>.
- [31] R. Abramishvili *et al.* (COMET collaboration), “COMET Phase-I technical design report”, *PTEP* **2020** (2020), no. 3, article ID 033C01.
- [32] Y. Kuno, (COMET collaboration), “A search for muon-to-electron conversion at J-PARC: the COMET experiment”, *Progr. Theoret. Exp. Progress* **2013** (2013), article ID 022C01.
- [33] Y. G. Cui *et al.* (COMET collaboration), “J-PARC PAC E21 Proposal”, 2009, unpublished.

- [34] J. C. Angélique *et al.* (COMET collaboration), “COMET – A submission to the 2020 update of the European Strategy for Particle Physics on behalf of the COMET collaboration”, 2018, preprint, <https://arxiv.org/abs/1812.07824>.
- [35] R. M. Dzhilkibaev, V. M. Lobashev, “On the search for $\mu \rightarrow e$ conversion on nuclei”, *Sov. J. Nucl. Phys.* **49** (1989), no. 2, p. 384-385.
- [36] S. Cook *et al.*, “Delivering the worlds most intense muon beam”, *Phys. Rev. Accel. Beams* **20** (2017), no. 3, article ID 030101.
- [37] Y. Kuno *et al.* (PRISM collaboration), J-PARC LOI, (2006), unpublished.
- [38] M. Pendlebury *et al.*, “Revised experimental upper limit on the electric dipole moment of the neutron”, *Phys. Rev. D* **92** (2015), article ID 092003.
- [39] J. Brod, U. Haisch, J. Zupan, “Constraints on CP-violating Higgs couplings to the third generation”, *JHEP* **1311** (2013), article ID 180.
- [40] J. Brod, E. Stamou, “Electric dipole moment constraints on CP-violating heavy-quark Yukawas at next-to-leading order”, 2018, preprint, <https://arxiv.org/abs/1810.12303>.
- [41] J. Brod, D. Skodras, “Electric dipole moment constraints on CP-violating light-quark Yukawas”, *JHEP* **1901** (2019), article ID 233.
- [42] J. M. Cline, “Is electroweak baryogenesis dead?”, *Philos. Trans. R. Soc. Lond. A* **376** (2018), no. 2114, article ID 20170116.
- [43] J. H. Smith, E. M. Purcell, N. F. Ramsey, *Phys. Rev.* **108** (1957), p. 120-122.
- [44] C. Abel *et al.*, “nEDM experiment at PSI: data-taking strategy and sensitivity of the dataset”, *EPJ Web Conf.* **219** (2019), article ID 02001.
- [45] www.psi.ch/nedm/edms-world-wide.
- [46] M. W. Ahmed *et al.*, “A new cryogenic apparatus to search for the neutron electric dipole moment”, *JINST* **14** (2019), no. 11, article ID P11017.
- [47] C. Abel *et al.*, “The n2EDM experiment at the Paul Scherrer Institute”, *EPJ Web Conf.* **219** (2019), article ID 02002.
- [48] T. M. Ito *et al.*, “Performance of the upgraded ultracold neutron source at Los Alamos National Laboratory and its implication for a possible neutron electric dipole moment experiment”, *Phys. Rev. C* **97** (2018), article ID 012501.
- [49] S. Ahmed *et al.* [TUCAN Collaboration], “First ultracold neutrons produced at TRIUMF”, *Phys. Rev. C* **99** (2019), article ID 025503.
- [50] A. Serebrov, “Present status and future prospects of n-EDM experiment of PNPI-ILL-PTI collaboration”, *PoS INPC2016* (2017), p. 179.
- [51] E. Chanel *et al.*, “The pulsed neutron beam EDM experiment”, *EPJ Web Conf.* **219** (2019), article ID 02004.
- [52] D. Wurm *et al.*, “The PanEDM neutron electric dipole moment experiment at the ILL”, *EPJ Web Conf.* **219** (2019), article ID 02006.